

We are IntechOpen, the world's leading publisher of Open Access books Built by scientists, for scientists

6,900

Open access books available

186,000

International authors and editors

200M

Downloads

Our authors are among the

154

Countries delivered to

TOP 1%

most cited scientists

12.2%

Contributors from top 500 universities



WEB OF SCIENCE™

Selection of our books indexed in the Book Citation Index
in Web of Science™ Core Collection (BKCI)

Interested in publishing with us?
Contact book.department@intechopen.com

Numbers displayed above are based on latest data collected.
For more information visit www.intechopen.com



Delineation of Open-Pit Mining Boundaries on Multispectral Imagery

Ioannis Kotaridis and Maria Lazaridou

Abstract

During the last decades, monitoring the spatial growth of open-pit mining areas has become a common procedure in an effort to comprehend the influence that mining activities have on the adjacent land-use/land-cover types. Various case studies have been presented, focusing on land-cover mapping of complex mining landscapes. They highlight that a rapid as well as accurate approach is critical. This paper presents a methodological framework for a rapid delineation of open-pit mining area boundaries. For that purpose an Object-Based Image Analysis (OBIA) methodology is implemented. Sentinel-2 data were obtained and the Mean-Shift segmentation algorithm was employed. Among the many methods that have been presented in literature in order to evaluate the performance of an image segmentation, an unsupervised approach is carried out. A quantitative evaluation of segmentation accuracy leads to a more targeted selection of segmentation parameter values and as a consequence is of utmost importance. The proposed methodology was mainly conducted through python scripts and may constitute a guide for relevant studies.

Keywords: OBIA, image segmentation, lignite mine, open-pit mining, Sentinel-2

1. Introduction

1.1 Mining activity and remote sensing

Mining comprises the activity that includes the extraction of geological materials from earth with tunnels, shafts or pits. Mining and mines can be classified in several ways. According to materials commonly mined, three classes of mining can be distinguished: metallic, non-metallic and fuel minerals. Based on the nature of excavation, mineral extraction can be categorized into two classes: underground and surface mining. The latter includes open-pit mining (also known as open-cast mining) that is implemented to extract deep and massive deposits that are not covered by a thick overburden. Underground mining of such deposits would be disadvantageous, since the material is mainly close to the surface [1].

Greece has been commonly included in the top lignite producers in Europe [2]. Mining of fuel minerals constitutes a critical activity, since a large percentage of the country's energy needs is covered by a solid fuel, lignite. The first lignite mine in Greece appeared in 1873, whereas systematic exploitation commenced after

1950. Nowadays, the primary lignite extraction basins are located in Ptolemaida and Amyntaio. Lignite exploitation in Greece is conducted by surface mining and specifically open-pit mining [3].

Mining and specifically coal mining activities may cause severe environmental impacts [4]. Landscapes formed by mining activities are vulnerable to several geomorphic hazards, for instance, landslides and rockfalls [1]. The stability of excavations is a critical aspect of Greek lignite mines which become larger and deeper in comparison with those in the past. During the last few years, many events of severe deformations and disastrous slope failures occurred [2]. In addition, flood is a probable hazard, since water can enter pits and tunnels [1]. Surrounding areas are affected by mining with economic, environmental and social impacts [5].

Taking into consideration their synoptic coverage and multitemporal data acquisition capabilities, remote sensing methods have been widely implemented in applications related to mining activities. Availability of high spatial resolution data resulted in an increased interest of using satellite data to monitor surface mining activities [4]. Remote sensing offers a valuable tool for acquiring rigorous data, while decreases the cost of field surveys both in time and money [6].

Remote sensing applications related to mining activities include the following: mapping of the surface mineralogy, topography and related changes that are quite valuable throughout the operation and planning of mine, identifying and monitoring environmental effects and mapping surface movements of mine structures in order to monitor safety features [7]. Furthermore, the size and location of mine areas as well as land-cover changes due to mining can be extracted from satellite images [5]. Remote sensing can make mine planning procedures easier, enhance safety during and after mine operation and monitor environmental effect as well as rehabilitation [7].

1.2 Image segmentation in OBIA

In contrast with traditional pixel-based approaches, the primary methodological component in Object-Based Image Analysis (OBIA) is the image object [8, 9]. OBIA produces meaningful image objects only if the imagery is partitioned into similar or relatively similar areas. This requires a low value of internal heterogeneity regarding the parameter that is examined in comparison with its adjoining areas [8].

Image segmentation is the first but also fundamental procedure to produce the core elements of OBIA [10]. It is about the partitioning of an image into spatially adjoining and homogenous groups of pixels (segments) that constitute the foundation for further analysis [8, 11]. These regions have similar spatial and spectral features, which, if considered as meaningful, depict a real-world object [9, 12]. By implementing image segmentation, the level of detail is decreased to make image content more comprehensive by lessening image complexity [9]. By transitioning from pixel to image object-based framework, in an effort to follow the example of visual interpretation, better management of spatial information can be accomplished, thus a more beneficial integration with Geographic Information System (GIS) can be achieved [13].

During the last decades, several segmentation methods were matured and employed in remote sensing applications [10]. Commonly, segmentation methods are classified into three broad categories: pixel-based, edge-based and region-based methods [14]. The selection of segmentation method is substantially influenced by the objective of image analysis study and it is typically acknowledged that it does not exist a perfect algorithm that will demonstrate adequate results with every satellite image. It has to be mentioned that most segmentation methods do not instantly produce meaningful image objects. However, clusters are generated with

generic labels, for example, region A, region B, etc. Then, these clusters have to be converted to meaningful image objects through a post-segmentation process [15].

A fairly demanding task in image segmentation procedure is the selection of segmentation parameters' values in order to generate segments that will comply with the needs of user and the purpose of study [10]. Since there is not a commonly accepted method to determine optimal segmentation parameters' values, image segmentation continues to be an interactive procedure that includes trial-and-error approaches.

A typical OBIA approach includes two main steps, image segmentation and object classification. On the other hand, there are studies that propose a methodology that includes only the step of image segmentation. It has to be noted that the application objective is the definitive factor concerning the methodology implemented. This study does not follow the traditional OBIA approach.

1.3 Relevant studies

Several studies have utilized satellite data and remote sensing methods to investigate an issue related to mining activities. Monitoring and evaluating reclamation procedure in mining areas is a common application [16]. LaJeunesse Connette et al. [17] developed a methodology to detect mining areas and evaluate mining expansion in Myanmar. For this reason they used data free of charge and open-source software. Likewise, Li et al. [18] employed multitemporal Landsat data to monitor the expansion of coal mining activity. Demirel et al. [6] proposed a methodology for detecting land use changes in surface coal mines with the use of multi-temporal high-resolution satellite data. Similarly, Guan et al. [19] investigated land use changes in a surface coal mine area located in the northeast China. In addition, Latifovic et al. [20] presented a methodology for land-cover change evaluation in the Athabasca Oil Sands region, northeast Alberta, Canada. For this purpose Landsat data were obtained. Maxwell et al. [21] combined very high resolution imagery and LIDAR data for mapping land-cover of a surface coal mine area in the southern coalfields of West Virginia, USA. Demirel et al. [22] investigated the potential implementation of a machine learning classifier (Support Vector Machines) for classifying high spatial resolution multispectral data of an open-cast mine area. Lechner et al. [23] carried out a spatial assessment of mine disturbance and rehabilitation of an open-pit mining study area. Townsend et al. [24] presented a methodology for quantifying land-use and land-cover change patterns due to surface mining and reclamation in the Central Appalachian Mountain region of the Eastern U.S., during a 30-year timeframe.

1.4 Scope of the study

The primary objective of the present work is to provide an object-based methodology for rapid detection and delineation of an open-pit mining area boundaries located nearby Amyntaio town, in northwestern Greece. Since image segmentation quality is a critical part in our analysis, an unsupervised evaluation of image segmentation performance was conducted, quantifying the internal homogeneity of segments and between segment separability.

2. Study area and data

The study area that was selected for this paper covers the Public Power Corporation (PPC) SA Amyntaio lignite mine. It has an extended mining history

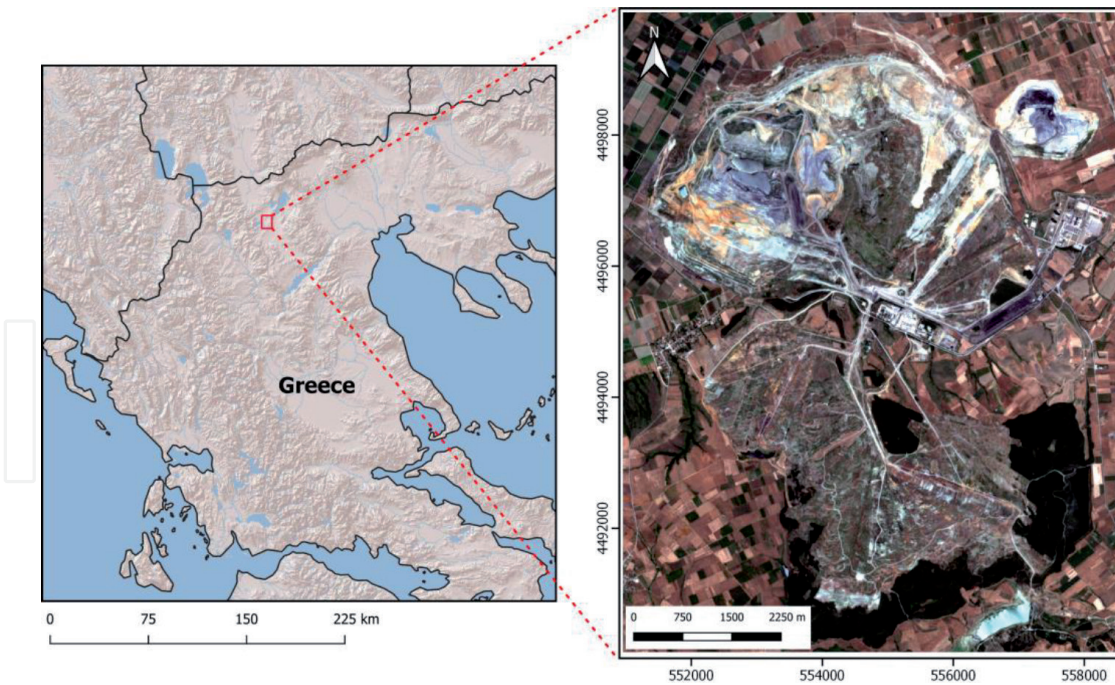


Figure 1. Study area located in Greece (left) and the subset of Sentinel-2A imagery (2020) (right).

that includes opencast mining with depths that reach 180 m, since the mid-1980s and is considered a critical mine for energy production in Greece. It is located in the north west part of mainland Greece. A subset was extracted from the main scene for analysis in order to include the mining operations as it appears in **Figure 1**, that is presented below.

In this paper Sentinel-2A, Level 2A (Bottom-Of-Atmosphere) corrected reflectance imagery was obtained. The scene acquisition date is 30 June 2020 (Tile T34TEK). The criteria for the selection of scene were limited cloud coverage and high quality.

3. Methodological procedure

The methodology implemented in order to delineate the boundaries of this open-pit mining area is presented in **Figure 2**.

3.1 Tools

Orfeo Toolbox (OTB) was used for digital processing of the imagery. It is an open-source project that supports processing of remote sensing data including high resolution optical, multispectral and radar images [25]. The algorithms utilized for the purpose of this study were accessed from Python through the `otbApplication` module. Spatial analysis procedures were carried out in QGIS, a free and open-source Geographic Information System that supports the creation, editing visualization and publication of geospatial data [26].

3.2 Initial processing of data

Initial processing of Sentinel-2A imagery includes resampling the 20 m bands to 10 m, clipping the scene to the boundaries of Area Of Interest (AOI) and concatenating the spectral bands to produce a single stacked image.

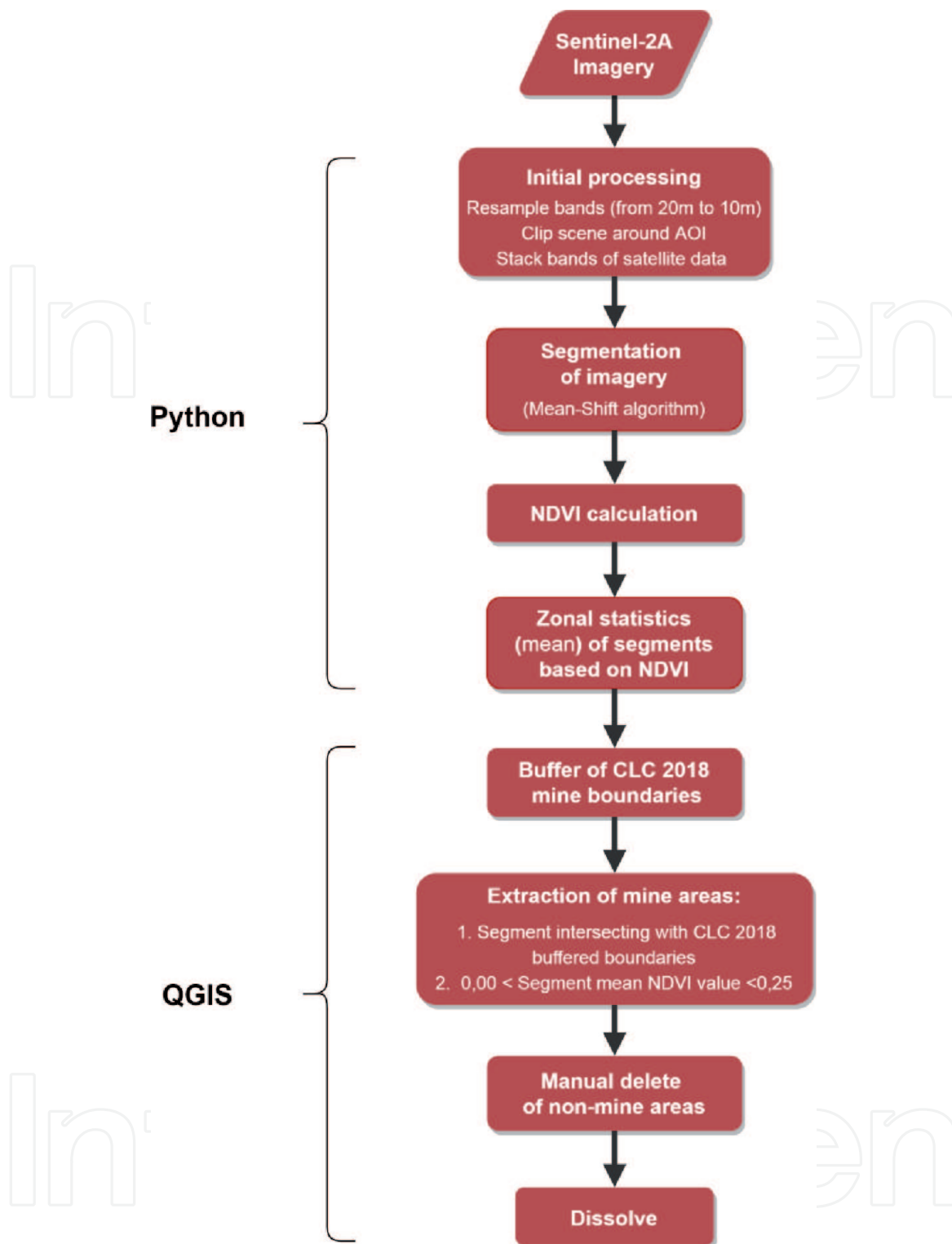


Figure 2.
Methodological framework.

3.3 Image segmentation

The stacked image was used as input for image segmentation. For the purpose of this study, Mean-Shift segmentation algorithm was implemented. It is a non-parametric clustering approach that is widely utilized in image analysis [27]. Mean-Shift segmentation algorithm has depicted adequate results regarding object extraction [28, 29]. It can handle different remote sensing satellite data, for instance, medium or high spatial resolution images. Critical factors that are related to its popularity are the simplicity of filtering step, the multivariate nature and the

existence of various implementations [30]. The vector output of segmentation and the selected parameter values of Mean-Shift algorithm are presented in **Figure 3**.

As shown in **Figure 3**, range radius and minimum region size parameter values were increased drastically compared to default values. This is necessary in order not to confuse mine areas with different land-cover types and not to have a large number of segments, so that they are manageable.

3.4 Evaluation of segmentation

A qualitative evaluation of segmentation output is commonly implemented through visual assessment [31]. This is a rather subjective mean of segmentation accuracy evaluation. Conversely, several supervised and unsupervised approaches

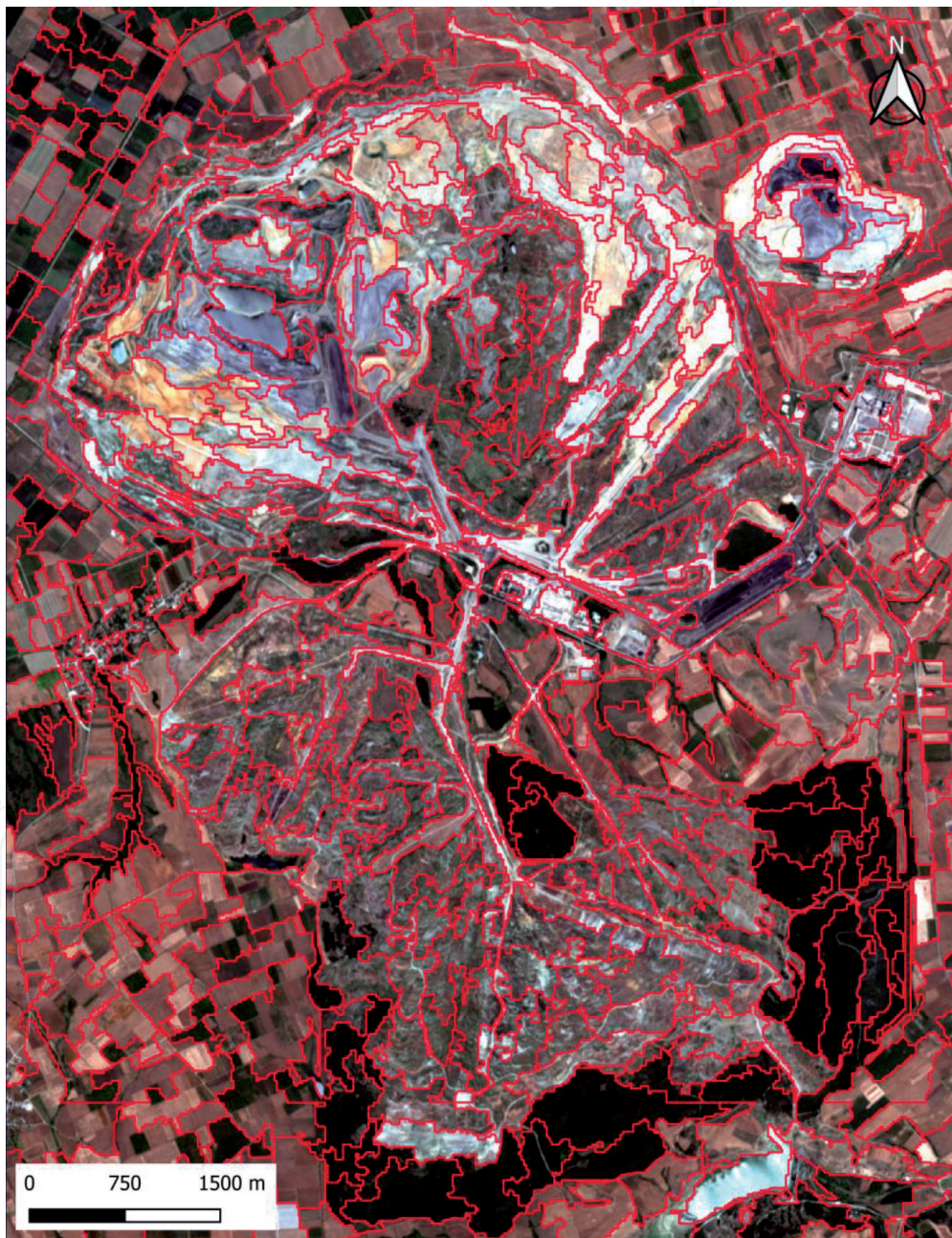


Figure 3. Segmentation results. The boundaries of segments are symbolized with red color (spatial radius: 4, range radius: 160, minimum region size: 700).

have been presented in order to assess image segmentation accuracy. Supervised methods typically compare segmentation output with a reference layer and measure the overlapping area [32]. Unsupervised approaches measure particular features of segments, for example, spectral homogeneity and between object heterogeneity [33]. However, there is not a standard methodology [32].

For the purpose of this study, an unsupervised approach was selected. In specific, the objective function proposed by Espindola et al. [33] was calculated to evaluate the quality of image segmentation results. This function consists of a measure of intrasegment homogeneity and one of intersegment heterogeneity. The first part is intrasegment variance of segments, a weighted average, where the area of each segment represents the corresponding weight. Thus, probable variabilities produced by smaller segments are eliminated. Furthermore, in order to evaluate intersegment heterogeneity, the function employs Moran's I autocorrelation index [34] that measures the spatial association as derived from the total of segments. Moran's I reflects how, on average, mean values of each segment vary from mean values of its adjacent segments. Small values of Moran's I suggest low spatial autocorrelation, hence the adjacent regions are statistically different. This denotes large intersegment heterogeneity. In other words, image segmentation produces segments with discrete boundaries. Employing spatial autocorrelation for evaluating image segmentation quality is especially suitable for region growing algorithms that generate closed polygons [33].

An adequate selection of parameters' values incorporates low intersegment Moran's I index with low intrasegment variance. The proposed function from Espindola [33] adds the normalized values of variance and autocorrelation measures. The objective function and its components were computed for each spectral band of Sentinel-2 imagery. Following, the value of objective function for the entire imagery was calculated by averaging the values of each spectral band. The results are presented in **Table 1**.

As shown in **Table 1**, the mean normalized value of variance slightly changes for different parameters' values and the lowest values corresponds to the lowest values of range radius and minimum region size, as expected. Moran's I index value is decreasing when range radius value and minimum region size are increasing, which means that segments get larger in size but also fewer in number. The selected Mean-Shift parameters' values for this specific study area

Mean-Shift parameters' values (Spatial radius/Range radius/Minimum region size)	Variance	Moran's I index	Objective function
5/15/100	0.53	0.57	1.10
4/80/700	0.59	0.38	0.97
4/120/700	0.60	0.35	0.95
4/160/700	0.60	0.34	0.95
4/200/700	0.60	0.38	0.98
4/240/700	0.59	0.36	0.95
4/200/1500	0.61	0.27	0.89
4/300/2000	0.59	0.28	0.87

Table 1.
The values of variance, Moran's I index and objective function for specific Mean-Shift parameters' values.

(4/160/700) correspond to relatively low Moran's I index value which denotes that neighboring segments are statistically discrete.

3.5 NDVI calculation

Normalized Difference Vegetation Index (NDVI) was computed among several spectral indices. The relevant bands for NDVI are Red and NIR. NDVI is a simple but also undoubtedly effective and extensively implemented index for quantifying green vegetation. NDVI values range from -1 to $+1$. Negative values suggest the existence of water bodies. Values close to zero (-0.1 – 0.1) typically correspond to barren land. Values above 0.1 commonly indicate the existence of green vegetation [35]. NDVI of the study area is presented in **Figure 4**.

As shown in **Figure 4**, values from 0 to 0.2 clearly indicate the existence of mine areas, as it can be visually recognized from the natural color image. This

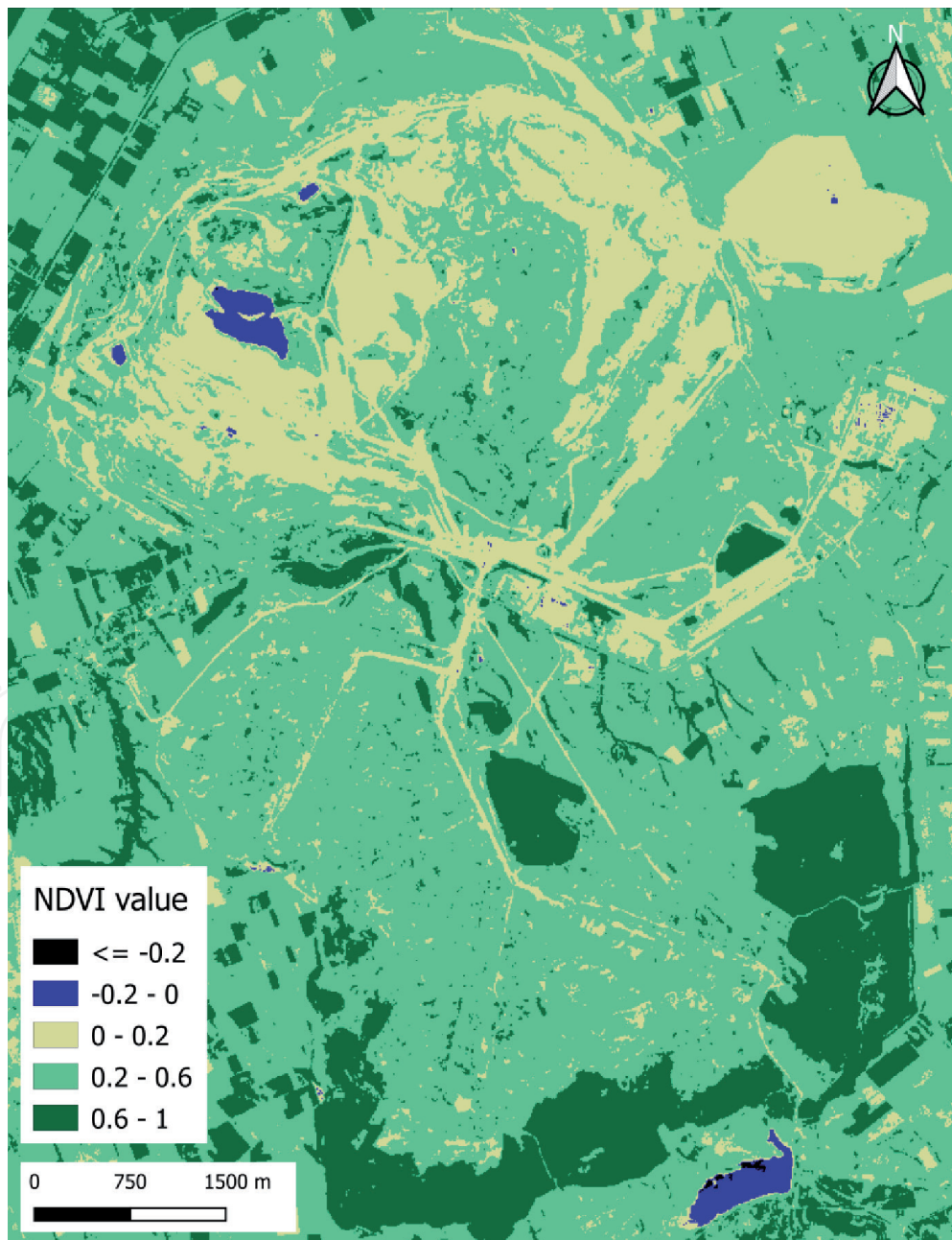


Figure 4.
NDVI of the imagery.

observation lead to the exploitation of this specific feature to extract the boundaries of mine areas.

3.6 Zonal statistics

Zonal statistics of segments were computed from NDVI raster layer. In specific, min, max, standard deviation and mean statistics were calculated over each segment. Following, they were exported in a vector layer (shapefile). It was ascertained that mean value statistic comprise an ideal indicator to identify mine areas. Mean value of NDVI for each segment is presented in **Figure 5** superimposed on the natural color image of the study area.

3.7 Delineation of mine area

Following the identification of mine areas, isolation of these areas is the next step. Since some areas outside mines share the same mean NDVI values with mines,

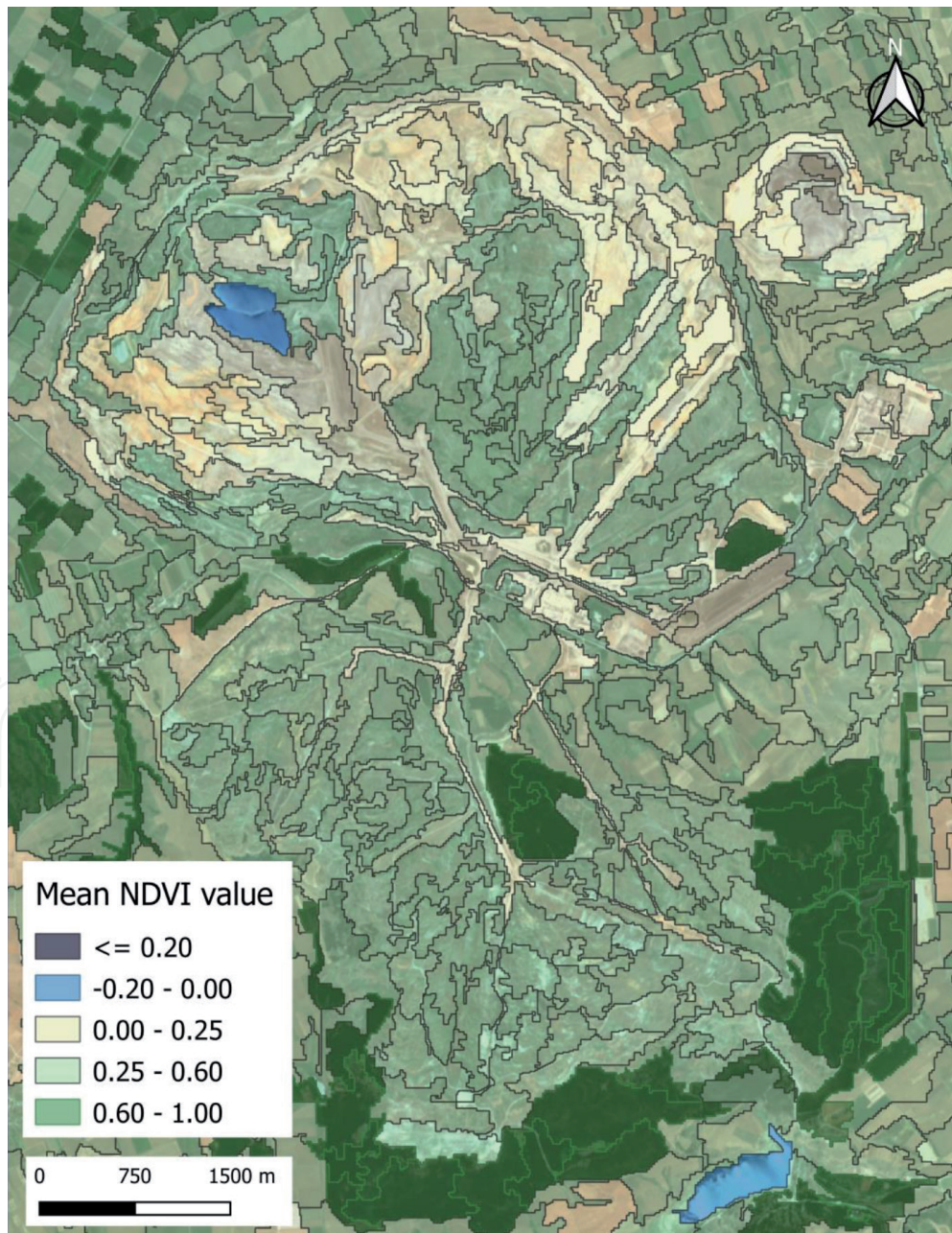


Figure 5.
Mean NDVI value of segments.

further processing of the vector layer is required. A dataset with rough boundaries of mine areas forms an auxiliary layer that can help to remove non-mine areas. In specific, Corine Land Cover (CLC) 2018 polygon of mine class was employed. A buffer area was computed using a fixed distance of 500 m for two main reasons. Minimum mapping unit of CLC datasets is 25 hectares, thus it is not appropriate for the scale of the analysis of this study and cannot be used unchanged. In addition, the reference year of satellite data used for the production of the latest CLC status layer is 2018, while the reference year of the imagery used in this paper is 2020. Several changes regarding mine boundaries occurred during this timeframe. CLC 2018 mine polygon and 500 m buffered polygon are presented in **Figure 6**.

A segment, in order to be characterized as mine area has to satisfy two conditions. It has to intersect with CLC 2018 buffered boundaries and its mean NDVI value has to be in the range of 0.00 to 0.25. Through this approach, segments were filtered and non-mine areas (polygons outside buffer zone) were erased. Furthermore, a manual more precise removal of non-mine areas was carried out to the remaining segments. The final step includes the implementation of dissolve algorithm in order to dissolve adjacent segments that share a common boundary.

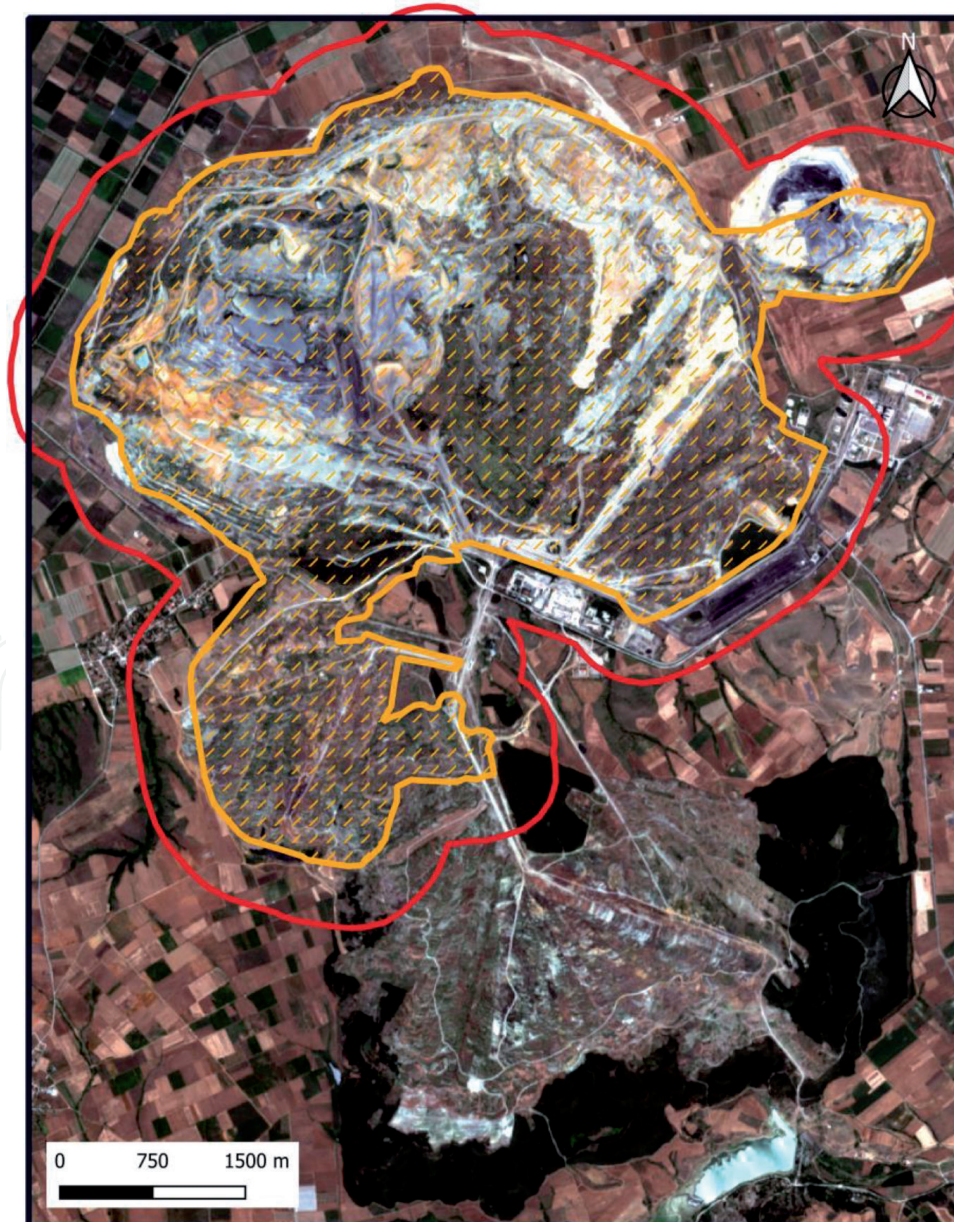


Figure 6.
CLC 2018 mine polygon (in orange color) and 500 m buffered polygon (in red color).

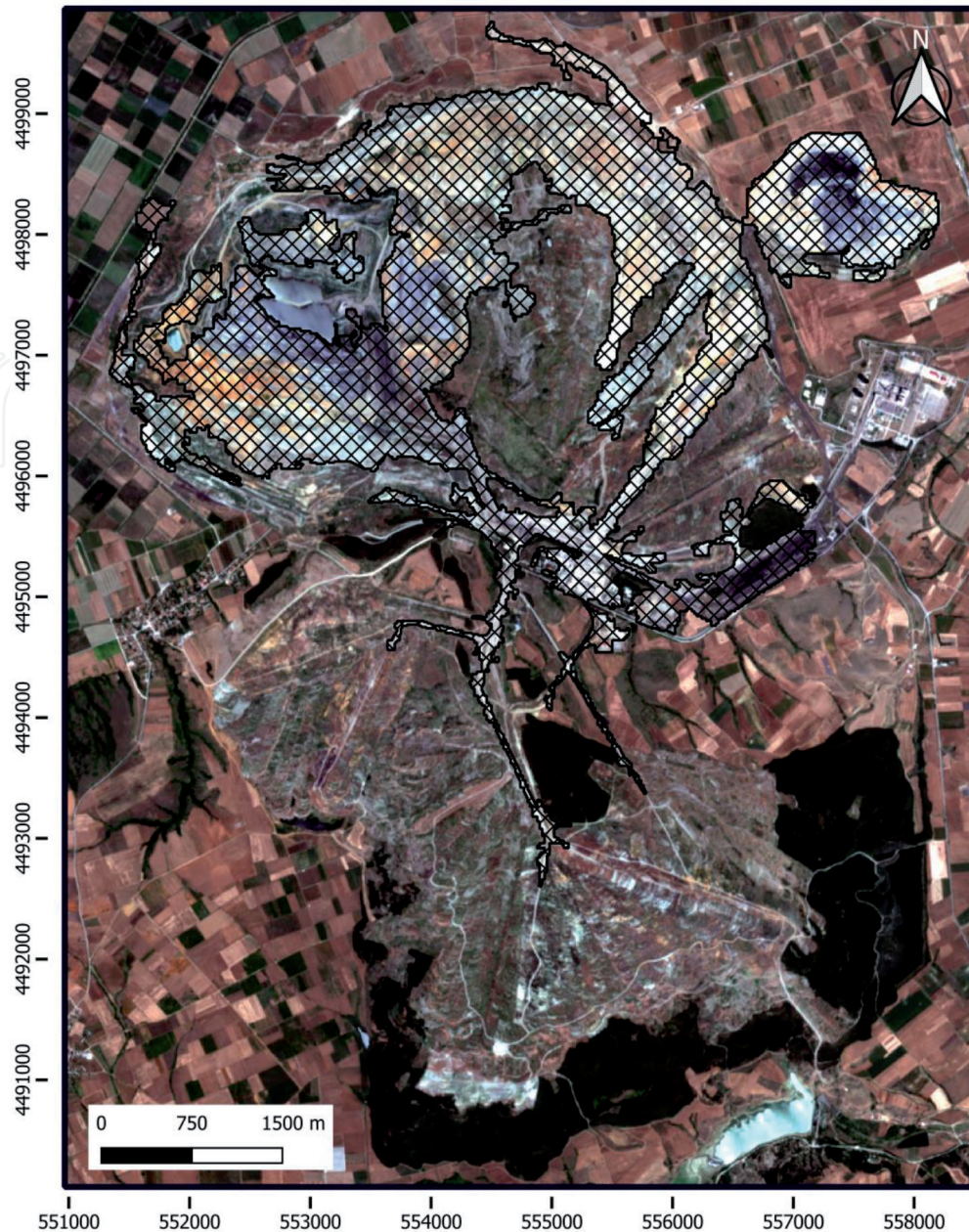


Figure 7.
Mine area in crosshatch pattern.

In this way, several segments were converted to a single meaningful image object (the mine area), that is demonstrated in **Figure 7**.

4. Discussion

An effective way of accomplishing adequate environmental management of mining areas requires the integration of remote sensing methods and Geographic Information Systems. Remote sensing provides image analysis fundamentals while a Geographic Information System offers spatial data analysis and geo-visualization tools. If these are exploited in a proper way, then continuous monitoring of mining activity can lead to efficient reclamation. In addition, freely-available data and open-source software drastically facilitates the efforts in this direction. This study utilized both of them in an effort to develop a comprehensive and at the same time rapid methodology for identifying mining areas and precisely delineating their boundaries. Of course, this approach can be beneficial for a multitemporal analysis in order to evaluate mining expansion.

The implemented approach for image segmentation evaluation that is demonstrated in this study does not require ground truth data, since it is an unsupervised method that is characterized by two features included in the following. Each segment should be internally homogeneous (weighted variance metric) and at the same time discrete from its adjacent segments (Moran's I spatial autocorrelation index). These two indicators are calculated for each spectral band and then combined into a global evaluation metric, the objective function. The main advantage of this approach is its robustness, since it exploits well-established statistical methods. However, since it is a global evaluation metric, it may not perform well when two segmentation results depict very similar performance but have dissimilar local error distributions. An approach that is capable of quantifying both locally and globally segmentation performance may be more suitable for the aforementioned situation.

5. Conclusion

In this study a methodology for rapid identification of mines and precise delineation of their boundaries is presented, with the use of both freely-available data and open-source software. For this reason a cloudless Sentinel-2A imagery was obtained covering the area of interest. Following the initial processing steps, image segmentation was carried out using Mean-Shift algorithm and an unsupervised segmentation evaluation metric was calculated for different parameters' values. It is combined by an autocorrelation index that identifies separability between segments and variance, an indicator that depicts the global homogeneity of segments. Then, NDVI and its mean values for each segment were computed. Finally, the mine area was extracted by implementing some spatial analysis tools including dissolve algorithm in order to aggregate segments that share a common boundary.

IntechOpen

Author details

Ioannis Kotaridis* and Maria Lazaridou
Laboratory of Photogrammetry - Remote Sensing, Faculty of Engineering, School of Civil Engineering, Aristotle University of Thessaloniki, Thessaloniki, Greece

*Address all correspondence to: iskotarid@civil.auth.gr

IntechOpen

© 2020 The Author(s). Licensee IntechOpen. This chapter is distributed under the terms of the Creative Commons Attribution License (<http://creativecommons.org/licenses/by/3.0>), which permits unrestricted use, distribution, and reproduction in any medium, provided the original work is properly cited. 

References

- [1] Mossa J, James LA. 13.6 Impacts of Mining on Geomorphic Systems. In: *Treatise on Geomorphology* [Internet]. 2013. p. 74-95. Available from: <https://linkinghub.elsevier.com/retrieve/pii/B9780123747396003444>
- [2] Zevgolias IE, Deliveris AV, Koukouzas NC. Slope failure incidents and other stability concerns in surface lignite mines in Greece. *Journal of Sustainable Mining*. 2019 Nov;18(4):182-97.
- [3] MiningGreece. [Internet]. Available from: <https://www.mininggreece.com/mining-greece/minerals/coal/> [Accessed: 2020-08-01]
- [4] Rathore† CS, Wright R. Monitoring environmental impacts of surface coal mining. *International Journal of Remote Sensing*. 1993;14(6):1021-42.
- [5] Werner TT, Mudd GM, Schipper AM, Huijbregts MAJ, Taneja L, Northey SA. Global-scale remote sensing of mine areas and analysis of factors explaining their extent. *Global Environmental Change*. 2020;60.
- [6] Demirel N, Düzgün Ş, Emil MK. Landuse change detection in a surface coal mine area using multi-temporal high-resolution satellite images. *International Journal of Mining, Reclamation and Environment*. 2011;25(4):342-9.
- [7] REMOTE SENSING FOR THE MINING INDUSTRY. [Internet]. 2018. Available from: https://www.oulu.fi/sites/default/files/36/RESEM_EOReview.pdf
- [8] Blaschke T, Burnett C, Pekkarinen A. Image Segmentation Methods for Object-based Analysis and Classification. In: Jong SMD, Meer FDV, editors. *Remote Sensing Image Analysis: Including the Spatial Domain*. Dordrecht: Springer; 2004. p. 211-36.
- [9] Lang S. Object-based image analysis for remote sensing applications: modeling reality – dealing with complexity. In: Blaschke T, Lang S, Hay GJ, editors. *Object-Based Image Analysis*. Berlin, Heidelberg: Springer Berlin Heidelberg; 2008. p. 3-27. (Lecture Notes in Geoinformation and Cartography). Available from: http://link.springer.com/10.1007/978-3-540-77058-9_1
- [10] Cheng G, Han J. A survey on object detection in optical remote sensing images. *ISPRS Journal of Photogrammetry and Remote Sensing*. 2016;117:11-28.
- [11] Nussbaum S, Menz G. Object-based image analysis and treaty verification: new approaches in remote sensing - applied to nuclear facilities in Iran. New York, NY: Springer; 2008. 170 p.
- [12] Navulur K. *Multispectral Image Analysis Using the Object-Oriented Paradigm* [Internet]. CRC Press; 2006. Available from: <https://www.taylorfrancis.com/books/9781420043075>
- [13] Castilla G, Hay GJ. Image objects and geographic objects. In: Blaschke T, Lang S, Hay GJ, editors. *Object-Based Image Analysis*. Berlin, Heidelberg: Springer Berlin Heidelberg; 2008. p. 91-110. (Lecture Notes in Geoinformation and Cartography). Available from: http://link.springer.com/10.1007/978-3-540-77058-9_5
- [14] Blaschke T, Hay GJ, Kelly M, Lang S, Hofmann P, Addink E, et al. Geographic Object-Based Image Analysis – Towards a new paradigm. *ISPRS Journal of Photogrammetry and Remote Sensing*. 2014;87:180-91.
- [15] Thenkabail PS, editor. *Remotely Sensed Data Characterization, Classification, and Accuracies*

- [Internet]. Boca Raton, Florida: CRC Press; 2015. Available from: <https://www.taylorfrancis.com/books/9781482217872>
- [16] Karan SK, Samadder SR, Maiti SK. Assessment of the capability of remote sensing and GIS techniques for monitoring reclamation success in coal mine degraded lands. *Journal of Environmental Management*. 2016;182:272-83.
- [17] LaJeunesse Connette K, Connette G, Bernd A, Phyo P, Aung K, Tun Y, et al. Assessment of Mining Extent and Expansion in Myanmar Based on Freely-Available Satellite Imagery. *Remote Sensing*. 2016;8(11):912.
- [18] Li N, Yan CZ, Xie JL. Remote sensing monitoring recent rapid increase of coal mining activity of an important energy base in northern China, a case study of Mu Us Sandy Land. *Resources, Conservation and Recycling*. 2015 Jan;94:129-35.
- [19] Guan C, Zhang B, Li J, Zhao J. Temporal and spatial changes of land use and landscape in a coal mining area in Xilingol grassland. *IOP Conf Ser: Earth Environ Sci*. 2017;52:012052.
- [20] Latifovic R, Fytas K, Chen J, Paraszczak J. Assessing land cover change resulting from large surface mining development. *International Journal of Applied Earth Observation and Geoinformation*. 2005;7(1):29-48.
- [21] Maxwell AE, Warner TA, Strager MP, Pal M. Combining RapidEye Satellite Imagery and Lidar for Mapping of Mining and Mine Reclamation. *photogramm eng remote sensing*. 2014;80(2):179-89.
- [22] Demirel N, Emil MK, Duzgun HS. Surface coal mine area monitoring using multi-temporal high-resolution satellite imagery. *International Journal of Coal Geology*. 2011;86(1):3-11.
- [23] Lechner AM, Kassulke O, Unger C. Spatial assessment of open cut coal mining progressive rehabilitation to support the monitoring of rehabilitation liabilities. *Resources Policy*. 2016;50:234-43.
- [24] Townsend PA, Helmers DP, Kingdon CC, McNeil BE, de Beurs KM, Eshleman KN. Changes in the extent of surface mining and reclamation in the Central Appalachians detected using a 1976-2006 Landsat time series. *Remote Sensing of Environment*. 2009;113(1):62-72.
- [25] Orfeo Toolbox. Open Source processing of remote sensing images [Internet]. 2020. Available from: <https://www.orfeo-toolbox.org/> [Accessed: 2020-08-01]
- [26] QGIS. A Free and Open Source Geographic Information System [Internet]. 2020. Available from: <https://qgis.org/en/site/> [Accessed: 2020-08-01]
- [27] Remote Sensing for Forest Cover Change Detection. Module 3: Introduction to QGIS and Land Cover Classification. [Internet]. 2016. Available from: https://servirglobal.net/Portals/0/Documents/Articles/ChangeDetectionTraining/Module3_LC_Classification_Accuracy_Assessment.pdf [Accessed: 2020-08-01]
- [28] Chehata N, Orny C, Boukir S, Guyon D, Wigneron JP. Object-based change detection in wind storm-damaged forest using high-resolution multispectral images. *International Journal of Remote Sensing*. 2014;35(13):4758-77.
- [29] Huang F, Chen Y, Li L, Zhou J, Tao J, Tan X, et al. Implementation of the parallel mean shift-based image segmentation algorithm on a GPU

cluster. *International Journal of Digital Earth*. 2019;12(3):328-53.

[30] Michel J, Youssefi D, Grizonnet M. Stable Mean-Shift Algorithm and Its Application to the Segmentation of Arbitrarily Large Remote Sensing Images. *IEEE Trans Geosci Remote Sensing*. 2015;53(2):952-64.

[31] Hurskainen P, Adhikari H, Siljander M, Pellikka PKE, Hemp A. Auxiliary datasets improve accuracy of object-based land use/land cover classification in heterogeneous savanna landscapes. *Remote Sensing of Environment*. 2019;233:111354.

[32] Costa H, Foody GM, Boyd DS. Supervised methods of image segmentation accuracy assessment in land cover mapping. *Remote Sensing of Environment*. 2018;205:338-51.

[33] Espindola GM, Camara G, Reis IA, Bins LS, Monteiro AM. Parameter selection for region-growing image segmentation algorithms using spatial autocorrelation. *International Journal of Remote Sensing*. 2006;27(14):3035-40.

[34] Fotheringham AS, Brunston C, Charlton M. *Quantitative geography: perspectives on spatial data analysis*. Sage; 2000.

[35] Custom-scripts. Normalized difference vegetation index [Internet]. 2017. Available from: <https://custom-scripts.sentinel-hub.com/sentinel-2/ndvi/> [Accessed: 2020-08-01]